J. Phys. G: Nucl. Part. Phys. **26** (2000) 1–9. Printed in the UK PII: S0954-3899(00)01225-1

Studies on inner bremsstrahlung from a few β-emitting isotopes

S L Keshava†‖, K Gopala‡ and P Venkataramaiah§

† Department of Radiation Physics, Kidwai Memorial Institute of Oncology, Hosur Road, Bangalore—560 029, India

‡ Department of Studies in Physics, Manasagangothri, Mysore—570 006, India

§ Kuvempu University, Shankaraghatta, Shimoga District, India

E-mail: root@kidwai.kar.nic.in

Received 25 January 1999

Abstract. Past experimental studies on the inner bremsstrahlung (IB) emission from the forbidden β transitions have shown marked deviations from the theoretical calculations of Lewis and Ford, Ford and Martin, Chang and Falkoff, Madansky and Gebhardt. In this paper we have re-analysed the data of IB emissions from four β-emitting isotopes, namely ^{89}Sr, ^{141}Ce, ^{111}Ag and ^{99}Tc, whose transitions are classified as forbidden. The raw experimental data already available in the literature are critically examined in the light of relevant statistics in order to arrive at meaningful conclusions. The unfolding of the IB spectra was done following the step-by-step procedure of Liden and Starfelt. The results obtained were different from those reported in the literature.

1. Introduction

Work on inner bremsstrahlung (IB) has been going on for many years, although it has become scarce of late. However, many of the differences observed between the theory and the experiments could not be explained until recently. The IB is a low-intensity continuous spectrum of electromagnetic radiation which accompanies all types of β decay. The theory for IB emission from allowed β transitions was deduced by Knipp and Uhlenbeck (1936) and independently by Bloch (1936), and is popularly known as the KUB theory. Chang and Falkoff (1949) (CF), Madansky *et al* (1951), Lewis and Ford (1957) (LF) and Gebhardt (1968) extended the KUB theory to include the forbidden character of β decay. LF incorporated a first-order approximation of the Fermi function. Ford and Martin (1969) (FM) added detour transition probability in addition to direct transition probability in forbidden transitions.

The experimental investigations on the IB emission from forbidden β transitions have shown marked deviations from theoretical predictions (Narasimhamurthy and Jnanananda 1967, Hakeem and Goodrich 1962, Persson 1965, 1964, Kreische *et al* 1968, Beatie and Byrne 1971, Narayana *et al* 1977, Prasad Babu *et al* 1976, Ricci 1958, Berenyi *et al* 1969). Common to all these studies is the fact that the later half of the IB intensity spectrum deviated positively from the theories. The higher the energy, the higher was the magnitude of deviation. Replacement of the first-order approximation by the exact Fermi function in the IB theories by Keshava *et al* (1997) did not appreciably bridge the gap between the theory and the experiment. In this paper we have tried to investigate the reasons for the reported higher intensities at the

‖ Author for correspondence.

0954-3899/00/010001+09$30.00

high-energy end of the IB spectrum in a few forbidden transitions. We have re-investigated IB spectra from several isotopes out of which four are presented here, namely ^{89}Sr, ^{141}Ce, ^{111}Ag and ^{99}Tc. The raw experimental data have been taken from published literature. It was found that the root of many of the discrepancies lies in the counting statistics as well as in the spectrum correction procedures, as we discuss later in this paper.

^{89}Sr[$(\frac{5}{2})^+$] β-decays to ^{89}Y[$(\frac{5}{2})^-$] with a half-life of 51 days, log $ft = 9.4$ and end-point energy 1490 keV. The decay is classified as unique first-forbidden (Babu *et al* 1985a). ^{141}Ce[$(\frac{7}{2})^-$] β-decays to ^{141}Pr[$(\frac{7}{2})^+$]; 145.44 keV (70%), log $ft = 7$, β end-point energy 436 keV; $(\frac{5}{2})^+$ ground state (30%): log $ft = 7.8$, β end-point energy 581 keV with a half-life of 32.5 days. The ^{141}Ce emits a prominent τ line of energy 145.44 keV. The transition is classified as non-unique first-forbidden (Gundurao and Sanjeevaiah 1982). The decay scheme of ^{111}Ag can be found elsewhere (Basavaraju *et al* 1984). This decay is classified as first-forbidden. The half-life is 7.5 days with three branching ratios. The corresponding β end-point energies are 1028 keV (92%), 783 keV (1%) and 686 keV (7.1%). ^{111}Ag emits two prominent Γ lines (245.2 and 342.12 keV). ^{99}Tc[$(\frac{9}{2})^+$] β-decays to ^{99}Ru[$(\frac{5}{2})^+$] with a half-life of 2.1×10^5 years, log $ft = 12.3$ and β end-point energy of 292 keV. The transformation is classified as non-unique second-forbidden (Gundurao *et al* 1983).

The study of the IB spectra of ^{89}Sr by Belletti *et al* (1962) using a coincidence technique showed considerable excess below 500 keV. The results of Persson (1964) were in excess at medium and high energies. Babu *et al* (1985a) observed positive deviation from all the theories.

Gundurao and Sanjeevaiah (1982) measured IB photon emissions from ^{141}Ce and found positive deviations from the LF and FM theories towards the high-energy end of the spectrum.

The experimental findings of Basavaraju *et al* (1984) on the ^{111}Ag isotope showed large deviations from the LF and FM calculations beyond 600 keV.

A similar disagreement from all the theoretical calculations was reported by Gundurao *et al* (1983) from their measurements of the IB spectrum emitted by ^{99}Tc.

2. Re-analysis of published data

The raw experimental data used were from (i) Babu *et al* for ^{89}Sr, (ii) Basavaraju *et al* (1984) for ^{11}Ag, (iii) Gundurao *et al* for ^{141}Ce and ^{99}Tc.

The statistical strength of the data are determined by the statistical significance of the *difference* between the mean *source plus background* (BG) counts (X) and the mean BG counts (B). Noting that the nuclear counting follows a Poisson distribution which approaches normal or Gaussian distribution when the number of measurements is large, the distribution of *sample means* also follows the normal distribution and so too does the distribution of the difference between any two *sample means*. In any given channel both *source plus BG* and BG counts are considered as the *samples* of a population for the purpose of conducting the statistical test. The standard error σ for the distribution of the *difference between any two sample means* is given by

$$\sigma = \sqrt{[X + B]}.$$

Denoting the difference $X - B$ as I_{ib}, the statistic $t = I_{\mathrm{ib}}/\sigma$ determines the confidence level of I_{ib}, which can be read from the Standard Normal Curve Area Tables (Armitage and Berry 1994) for which mean $= 0$, standard deviation $= 1$ and t is given by the abscissae extending from $-\infty$ to $+\infty$. p is the ratio of the area under the standard normal curve lying between any given value of t and $t = \infty$ to that between $t = 0$ and $t = \infty$. The p-value corresponding to $t = I_{\mathrm{ib}}/\sigma$ determines the required confidence level.

(i) If $I_{ib} \geqslant 3\sigma$, then the IB intensity lies in the confidence interval between 95–100% ($p \leqslant 0.003$). The data can be considered to be *excellent*.

(ii) If $2\sigma \leqslant I_{ib} < 3\sigma$, then the IB intensity lies in the confidence interval between 95% and 99.7% ($0.003 < p \leqslant 0.05$). The data can be considered to be *good*.

(iii) If $1\sigma \leqslant I_{ib} < 2\sigma$, then the IB intensity lies in the confidence interval between 68% and 95% ($0.05 < p \leqslant 0.32$). The data can be considered to be *fair*.

(iv) If $I_{ib} < 1\sigma$, then, as the IB intensity lies within the confidence interval of 68% ($p > 0.32$), the data are considered to be statistically *poor* and the *null* hypothesis may be accepted (i.e., the difference between X and B is considered insignificant and both X and B are treated as sample means coming from the same population of counts, i.e. the BG).

If it is decided to accept the data up to a certain maximum value of p (for example, 0.32, 0.05 or 0.003 corresponding to the confidence intervals of 68–100%, 95–100% or 99.7–100%) which may correspond to some channel number, say N, then the counts in the $(N+1)$th channel can be treated essentially as BG only. This magnitude of counts may be subtracted from all channels. This is similar to correcting positive zero error in any measuring instrument. This procedure may also be termed *base line shift* (BLS).

The experimental data obtained from the isotope ^{89}Sr were *excellent* up to 610 keV, *good* from 610 to 725 keV and *fair* from 725 to 925 keV. The similar figures for ^{141}Ce are 309, 309–347, 347–394 keV and for ^{99}Tc are 176, 176–196, 196–204 keV. As for ^{111}Ag, sizeable counts (with a $\leqslant$0.3% confidence level) were present up to the end-point energy.

Even though efforts are made to maintain stability of the instruments by the experimentalists, long hours of counting, the fact of BG counts and *source* counts being recorded at different times and the fact that inherent fluctuations exist in both, make the difference counts I_{ib} either positive or negative towards the end-point energy where *nil* counts are expected. This fact also justifies the BLS described above.

In our present analysis, the data terminated at different levels of confidence were processed with and without BLS. The unfolding of the IB intensities from the raw data was carried out adopting the step-by-step procedure of Liden and Starfelt (1953), details of which can be found elsewhere (Basavaraju *et al* 1984, Babu *et al* 1985b). After initial BG subtraction and pile-up (PU) correction, the discrete Γ lines, if any, along with their Compton continua are subtracted using the knowledge of source activity, geometric detection efficiency of the detector and the peak-to-total ratio. The intensity spectrum is then corrected for the finite-energy resolution of the NaI (Tl) detector. The resolution function is taken as Gaussian. Next, the correction due to the Compton electron distribution is made. Further, the data are subjected to iodine-K x-ray escape correction and the geometric detection efficiency of the detector–source spatial configuration including the attenuation of photons by the aluminium covering of the detector and the β absorber (if used). Finally, the spectrum is corrected for the photo-peak efficiency of the detector.

However, it is necessary to mention the distortion caused by the detector resolution correction. The IB spectral data undergoing this correction tend to show false higher intensities in a few channels at the beginning and in a few channels towards the end. Due to the absence of counts on one side, the convolution procedure adds counts to these channels and hence the corrected data show false higher intensities. Apart from this, most of the spectrum is well corrected within two or three iterations.

3. Results and discussion

The experimental IB intensities after all corrections were converted to obtain the IB photon intensity per β/mc^2 energy range. The experimental results of ^{89}Sr are shown in figures 1 and 2. Figure 1 shows (i) the BG- and PU-corrected full raw data, (ii) the corresponding resolution-corrected data and (iii) the Compton electron distribution. Termination of data at different levels of confidence is not shown for clarity. Among the theoretical distributions, only the CF calculation for the second-forbidden transitions is shown in figure 2 as the experimental spectrum showed no agreement with the KUB, LF and FM theories. The experimental IB spectrum calculated using (i) full data with no BLS (NBLS), (ii) the data with $p \leqslant 0.32$ with NBLS and (iii) the data with $p \leqslant 0.32$ with BLS are also shown. All the experimental IB intensities are normalized with respect to the CF theoretical intensity at 700 keV. The effect of termination of data at some energy position and processing it without BLS is clearly demonstrated (i.e. the tendency of the IB curve to move upwards). Since the experimental data are statistically poor beyond 925 keV, the observed excesses over the theory in the later half of the energy range, as shown by the curve corresponding to the full data without BLS, cannot be taken seriously and no meaningful conclusion can be drawn from this part of the spectrum. That is, we have no statistical strength to conclude that the IB intensities are showing positive deviations from the theory. However, the shape of the experimental curves with and without BLS are close to the CF curve up to 800 keV as the BLS lowers the intensity in a few channels towards the end. On the basis of this trend, it may be concluded that the isotope exhibits the characteristics of a second-forbidden transition.

Figures 3 and 4 describe the results obtained for the ^{141}Ce isotope. Figure 3 shows (i) BG- and PU-corrected full raw data, (ii) resolution-corrected full data, (iii) resolution correction to data with $p \leqslant 0.32$ with NBLS, (iv) resolution correction to data with $p \leqslant 0.32$ with BLS and (v) Compton electron correction. Figure 4 shows the theoretical distribution due to both the LF (first-forbidden) and CF (second-forbidden) and also the experimental IB results (full data) normalized to CF at 356 keV. The shape of the experimental curve shows that the IB from ^{141}Ce exhibits the characteristics of a second-forbidden transition.

Figures 5 and 6 explain the experimental work on ^{111}Ag. Figure 5 gives (i) the BG- and PU-corrected raw IB spectrum along with source Γ lines, (ii) data after subtraction of source Γ lines from the BG- and PU-corrected raw data and (iii) Compton electron distribution. In figure 6, the theoretical spectrum due to CF (second-forbidden), LF and FM (first-forbidden with the exact Fermi function being used for Coulomb correction) are given along with the experimental curves (with NBLS as well as BLS) which are normalized at 450 keV to CF. There is no agreement with the LF and FM theoretical calculations. The IB spectrum processed with NBLS is seen to deviate positively whereas the one processed with BLS comes close to the CF theory.

Thus, the IB spectra from all three isotopes discussed above have shown the characteristics of second-forbiddenness although their transitions were classified as first-forbidden.

Lastly, figures 7 and 8 illustrate experimental results of ^{99}Tc. Figure 7 shows (i) the BG- and PU-corrected raw spectrum for data with $p \leqslant 0.32$, (ii) resolution-corrected data with NBLS, (iii) resolution-corrected data with BLS and (iv) Compton electron distribution. Figure 8 gives the experimental IB spectrum corresponding to the raw data in figure 7 (i.e. with NBLS as well as BLS). The theoretical spectrum due to LF (first-forbidden) alone is shown as there is no agreement with other theories. A good agreement between the experiment and the first-forbidden theory of LF is seen whereas the β decay of ^{99}Tc is classified as second-forbidden.

In conclusion, the hitherto observed discrepancies are perhaps due to the lacuna on the part

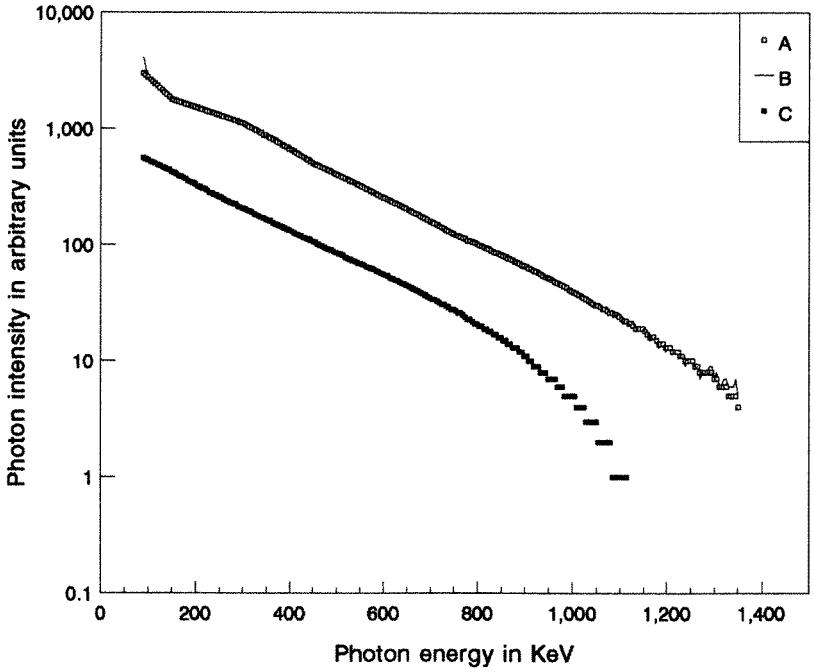

Figure 1. Raw experimental IB spectrum of ^{89}Sr. A, BG- and PU-corrected total spectrum; B, spectrum after resolution correction and C, Compton electron distribution.

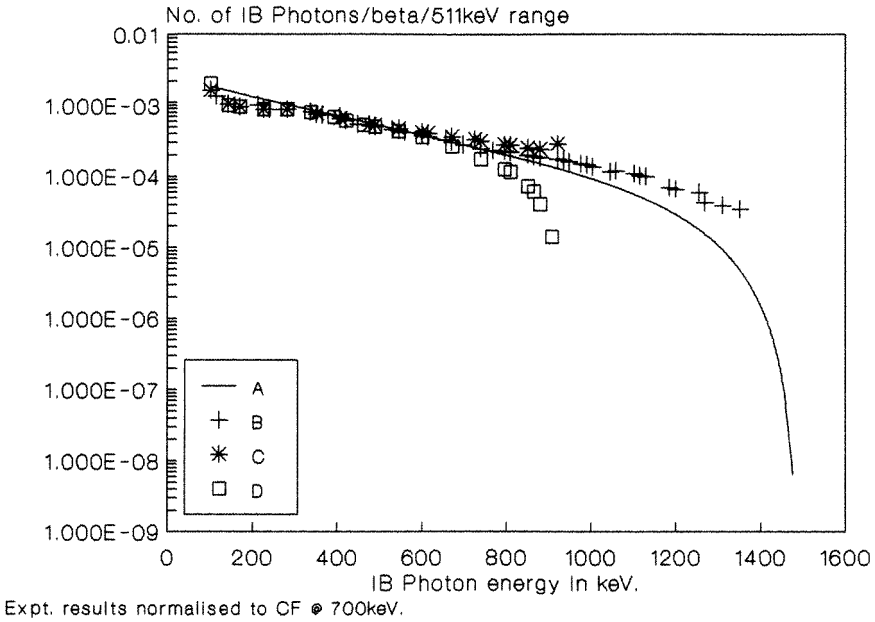

Figure 2. Comparison of experimental IB spectrum of ^{89}Sr after all corrections with theoretical spectrum. A, CF theoretical spectrum for second-forbidden β transitions. B, experimental IB spectrum corresponding to raw data in the confidence interval 0–100%. C, experimental IB spectrum corresponding to raw data within the confidence interval 68–100% ($p \leqslant 0.32$) processed with NBLS. D, experimental IB spectrum corresponding to raw data in the confidence interval 68–100% ($p \leqslant 0.32$) processed with BLS.

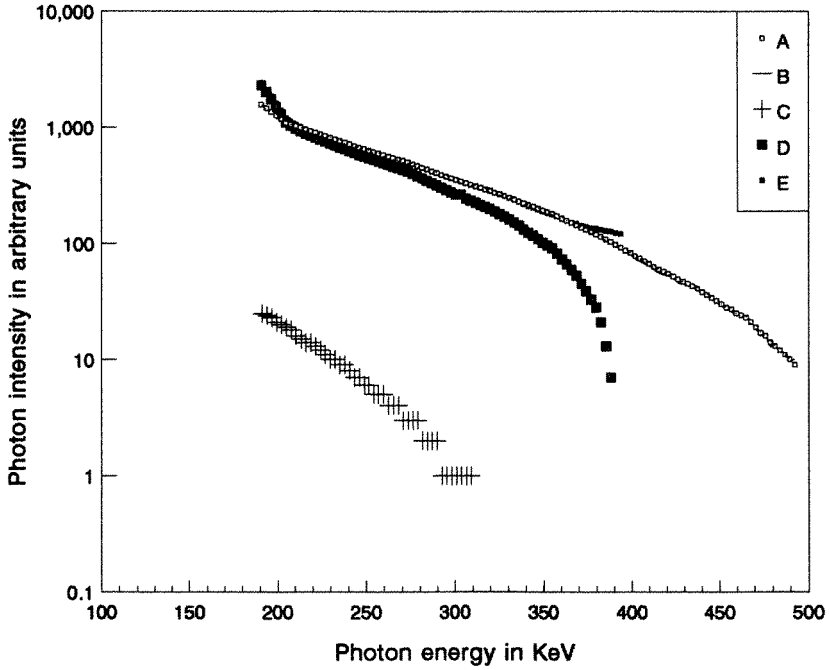

Figure 3. Raw experimental IB spectrum of ^{141}Ce. A, BG- and PU-corrected whole spectrum; B, whole spectrum after resolution correction; C, Compton electron distribution; D, resolution correction to the data limited to the confidence interval 68–100% ($p \leqslant 0.32$) with BLS; E, resolution correction to the data limited to the confidence interval of 68–100% ($p \leqslant 0.32$) with NBLS.

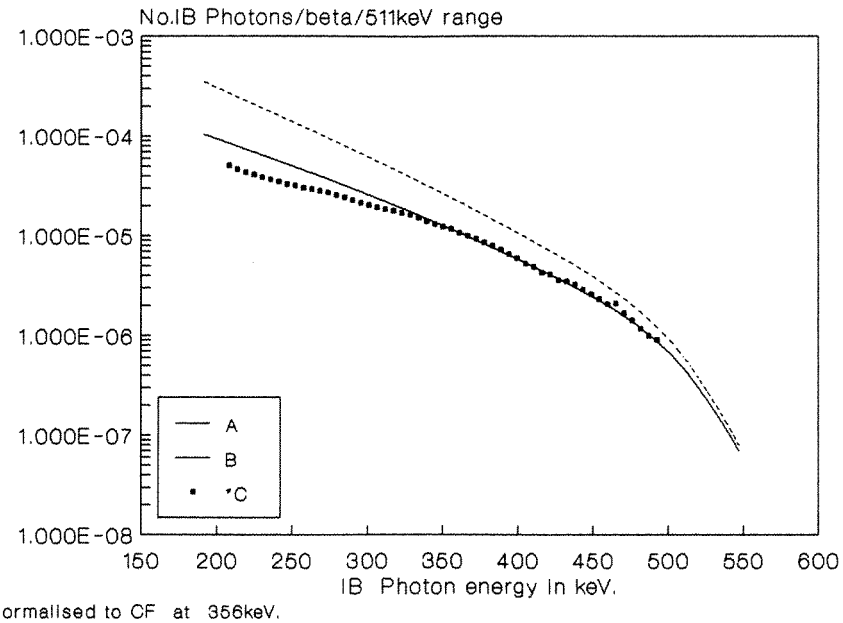

Figure 4. Comparison of experimental IB spectrum of ^{141}Ce with theory. A, CF theoretical IB spectrum for second-forbidden β transitions; B, LF theoretical IB spectrum for first-forbidden IB spectrum; C, experimental IB spectrum corrresponding to the raw data in the confidence interval 0–100%.

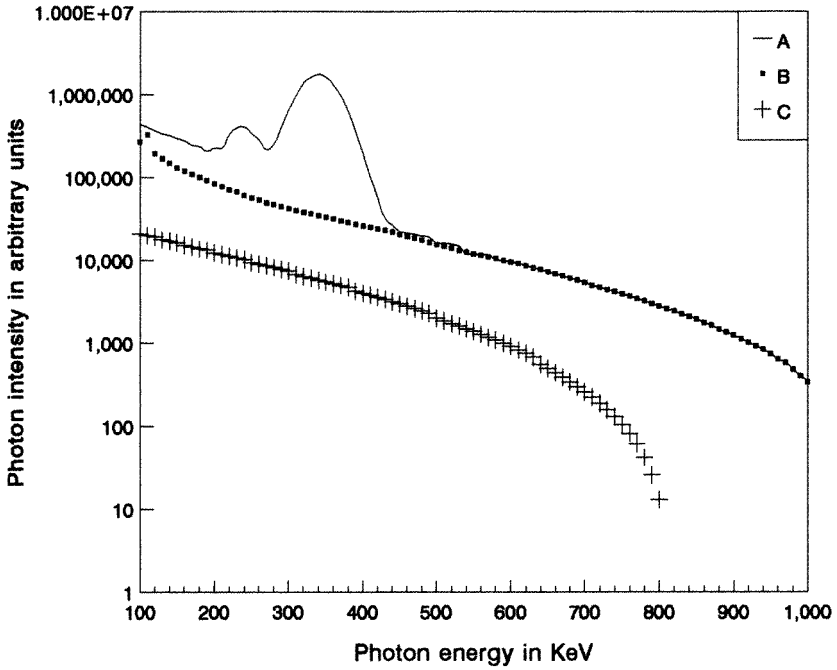

Figure 5. Raw IB spectrum of ^{111}Ag. A, BG- and PU-corrected spectrum of ^{111}Ag; B, the intensity curve after the subtraction of source τ lines; C, Compton electron distribution.

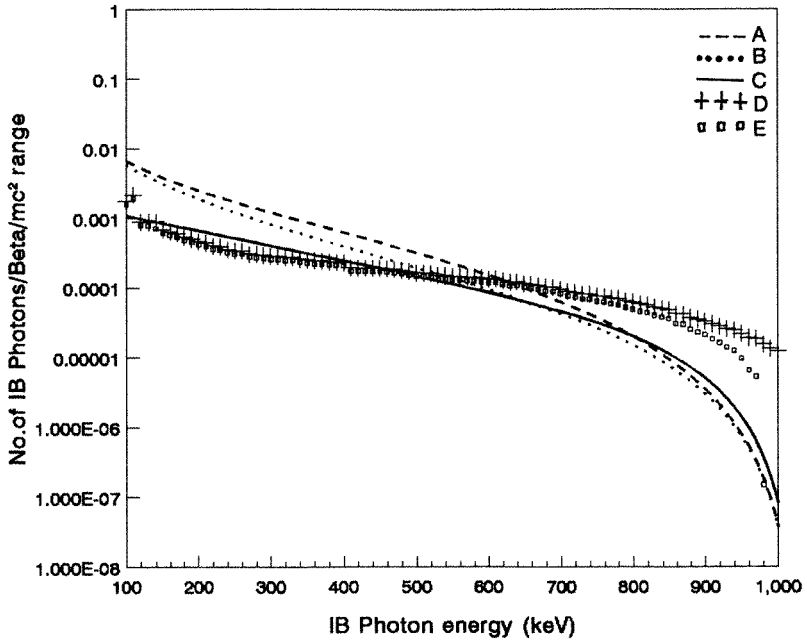

Figure 6. Comparison of the IB spectrum of ^{111}Ag with theory. A, FM; B, LF (first-forbidden) and C, CF (second-forbidden) theoretical distributions. D, experimental IB spectrum with NBLS. E, experimental IB spectrum with BLS.

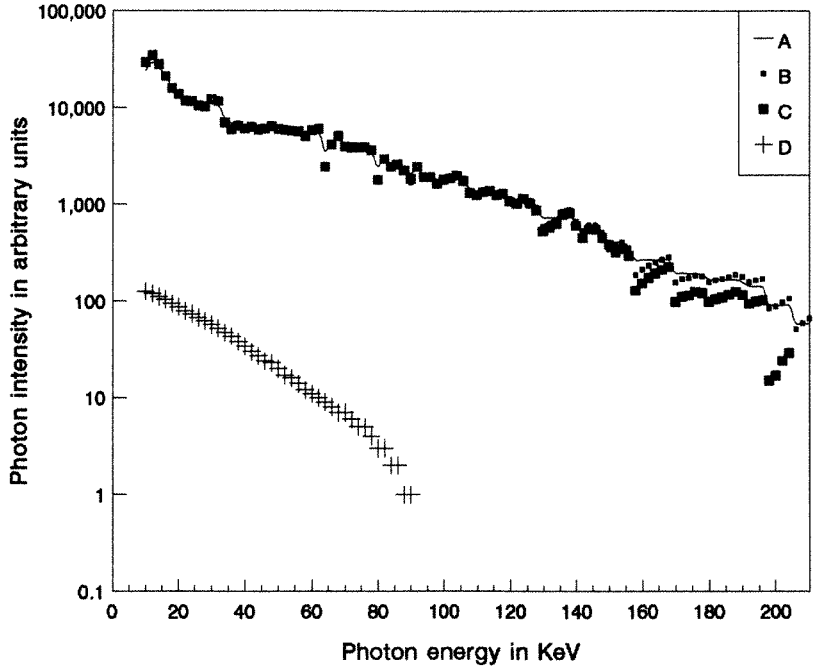

Figure 7. Raw IB spectrum of ^{99}Tc. A, BG- and PU-corrected spectrum. B, spectrum after resolution correction to the data in the confidence interval 68–100% ($p \leqslant 0.32$) with NBLS. C, spectrum after resolution correction to the data in the confidence interval 68–100% ($p \leqslant 0.32$) with BLS. D, Compton electron distribution.

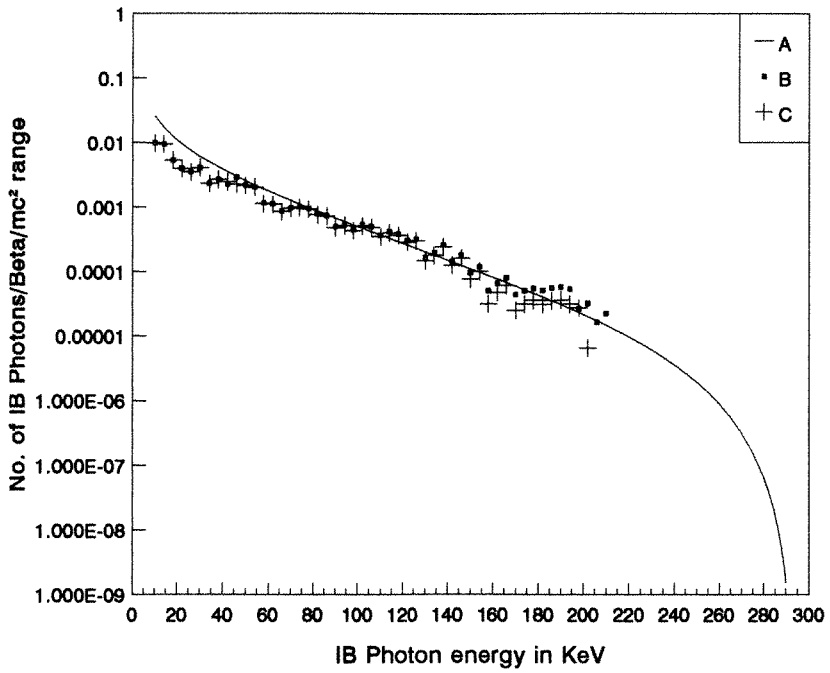

Figure 8. Comparison of experimental IB spectrum of ^{99}Tc with theory. A, LF theoretical IB spectrum for first-forbidden transitions. B, experimental IB spectrum corresponding to raw data in the confidence interval 68–100% with NBLS. C, experimental IB spectrum corrresponding to the raw data in the confidence interval 68–100% with BLS.

of the experimental set-up because of the inability to produce a BG-free laboratory environment and it may be the poor statistical strength of the count data towards the end-point energy position, which are responsible for the higher intensities at the high-energy end reported earlier. The BLS method described in this paper and careful treatment of the resolution correction at the extremities of the spectrum are likely to bring the theory and experiment closer to each other.

Acknowledgments

Thanks are due to the Kidwai Memorial Institute of Oncology, Bangalore, for computer facilities. One of us (KG) thanks the University Grants Commission for the Emeritus Fellowship.

References

Armitage P and Berry G 1994 *Statistical Methods in Medical Research* 3rd edn (Palo Alto, CA: Blackwell Scientific) pp 41–146

Babu B R S, Venkataramaiah P, Gopala K and Sanjeevaiah H 1985a *Proc 3rd Int. Symp. on Radiation Physics, University of Ferrara, Italy*

——1985b *J. Phys. G: Nucl. Phys.* **11** 1213

Basavaraju A, Venkataramaiah P, Gopala K and Sanjeevaiah H 1984 *J. Phys. G: Nucl. Phys.* **10** 563

Beatie J D and Byrne J 1971 *Nucl. Phys.* A **161** 650

Beletti S, Manduchi C, Nardelli G and Russo-Mancuchi M T 1962 *Nuovo Cimento* **25** 254

Berenyi D, Scharbert T and Vatai E 1969 *Nucl. Phys.* A **137** 80

Bloch F 1936 *Phys. Rev.* **50** 272

Chang C S and Falkoff D L 1949 *Phys. Rev.* **76** 365

Ford G W and Martin C F 1969 *Nucl. Phys.* A **134** 457

Gebhardt D 1968 *Nucl. Phys.* A **107** 593

Gundurao K S and Sanjeevaiah H 1982 *Nucl. Phys.* A **376** 478

Gundurao K S, Venkataramaiah P, Gopala K and Sanjeevaiah H 1983 *J. Phys. G: Nucl. Phys.* **9** 691

Hakeem M A and Goodrich M 1962 *Nucl. Phys.* **31** 322

Keshava S L, Gopala K, Venkataramaiah P and Gopinath D V 1997 *Indian J. Phys.* A **71** 481

Knipp J K and Uhlenbeck G E 1936 *Physica* **3** 425

Kreische W, Lampert W and Loos G 1968 *Nucl. Phys.* A **107** 601

Lewis R R and Ford G W 1957 *Phys. Rev.* **107** 756

Liden K and Starfelt N 1953 *Ark. Fys.* **7** 427

Madansky L, Lipps F, Bolgiano P and Berlin T H 1951 *Phys. Rev.* **84** 596

Narasimhamurthy K and Jnanananda S 1967 *Proc. Phys. Soc.* **90** 109

Narayana D G S, Narasimhamurthy K and Subrahmanyam V V V 1977 *Curr. Sci.* **46** 1

Persson B 1964 *Nucl. Phys.* **55** 49

——1965 *Nucl. Phys.* **67** 121

Prasad Babu R, Narasimhamurthy K and Narasimhamurthy V A 1976 *Phys. Rev.* C **13** 1267

Ricci R A 1958 *Physica* **24** 297